J Fluoresc (2009) 19:921–930
DOI 10.1007/s10895-009-0525-4

ORIGINAL PAPER

A Fluorescence Study of Novel Styrylindoles in Homogenous and Microhetrogeneous Media

Abera Asefa · Anil K. Singh

Received: 25 June 2007 / Accepted: 24 September 2007 / Published online: 11 August 2009
© Springer Science + Business Media, LLC 2009

Abstract In this paper are presented absorption and fluorescence emission properties of 3-styrylindoles *viz*. 3-(2-phenylethenyl-*E*)-NH-indole (**1**), 3-[2-(4-nitrophenyl) ethenyl-*E*)-NH-indole (**2**), 3-[2-(4-cyanophenyl)ethenyl-*E*]-N-ethylindole (**3**) and 3-[2-(4-cyanophenyl)ethenyl-*E*]-NH-indole (**4**) in organic solvents, 1,4-dioxane-water binary mixtures and micelles (SDS, CTAB and Triton-X-100). The fluorescence properties of **2**-**4** have been utilized to probe the microenvironment (binding constant, CMC, micro-polarity and solubilization site) of the micelles.

Keywords Styrylindoles · Fluorescence probe · Quenching · Micelle · Charge transfer

Introduction

Numerous fluorescent molecules are used as reporters of the microenviroments in complex biological systems or in simpler systems like organized assemblies of micelles [1–3]. However, the electron donor-acceptor molecules are generally the preferred ones because of the sensitivity of their intramolecular charge transfer (ICT) fluorescence on polarity of the media [4–6]. It has been reported that nitro-substituted styrylindoles exhibit solvent polarity dependent fluorescence emission from their conformationally relaxed intramolecular charge transfer (CRICT) excited state, which is considered to be a dipolar twisted state [7–10]. In the present work, we synthesized 3-styrylindoles namely 3-(2-phenylethenyl-*E*)-NH-indole (**1**), 3-[2-(4-nitrophenyl) ethenyl-*E*)-NH-indole (**2**), 3-[2-(4-cyanophenyl)ethenyl-*E*]-N-ethylindole (**3**) and 3-[2-(4-cyanophenyl)ethenyl-*E*]-NH-indole (**4**) (Fig. 1) and investigated their photophysical properties in homogeneous organic solvents and heterogeneous media of micelles (CTAB, SDS and Triton-X-100). This is to understand the effect of substituents on the excited state properties of 3-styrylindoles and further to explore their efficacy as fluorescence probe for organized assemblies, particularly of cationic, anionic and neutral micelles.

A. Asefa · A. K. Singh (✉)
Department of Chemistry, Indian Institute of Technology Bombay, Powai,
Mumbai 400 076, India
e-mail: retinal@chem.iitb.ac.in

Experimental

Indole was obtained from Spectrochem Pvt. Ltd., Mumbai and used without further purification. *p*-Nitrophenylacetic acid and benzenesulfonyl chloride were purchased from Sisco Research Laboratory Pvt. Ltd., Mumbai. Rhodamin B and quinine sulfate were purchased from Sigma-Aldrich. N-Bromosuccinimide (NBS) was obtained from LOBA Chemie Pvt. Ltd., Mumbai and was purified by recrystallization from water prior to use. Cetyltrimethylammonium bromide (CTAB), sodium dodecyl sulfate (SDS) and Ttiton-X-100 were purchased from Sisco Reasearch Laboratory, Mumbai, India and used as such without further purification. For quenching studies, AR grade hydrated copper sulfate and potassium iodide were obtained from Merck and Ronbaxy Laboratory Limited, respectively. All organic solvents were of AR or UV grade and further dried and distilled.

Melting points were determined by Veego melting point apparatus. FTIR spectra were recorded with Impact Nicolet-400 spectrophotometer using KBr method. ^{1}H NMR spectra were recorded with Varian VXR 400 MHz using

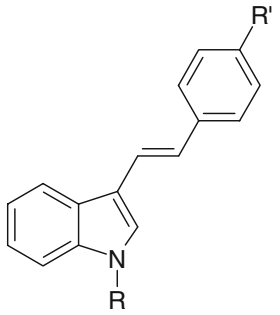

1 R = H R' = H
2 R = H R' = NO_2
3 R = C_2H_5 R' = CN
4 R = H R' = CN

Fig. 1 Structures of compounds **1**–**4**

TMS as internal standard. Mass spectrum was recorded with Micromass Q-TOF micro instrument. HPLC analyses were performed using Hitachi L-6250 intelligent pump attached to U-2000 spectrophotometer and using Lichrosorb analytical column. The absorption spectra were measured by JASCO V570 spectrophotometer. The fluorescence spectra were recorded on a Perkin Elmer LS-55 spectrofluorimeter by exciting at the absorption maxima ($\lambda_{ab\ max}$) and the excitation spectra were obtained by using the fluorescence emission maximum ($\lambda_{f\ max}$) of the respective compounds. The fluorescence quantum yields (Φ_f) at room temperature were measured relative to quinine sulfate in 0.1 N H_2SO_4 (Φ_f=0.51) [11] and rhodamin B (for compound **2**) in ethanol (Φ_f = 0.69) [12], and calculated by using the following equation [13].

$$\Phi = \Phi_{ref} \frac{n_{ref}^2}{n^2} \frac{OD_{ref}}{OD} \frac{A}{A_{ref}} \quad (1)$$

where n_{ref} and n are the refractive indices of the solvents, OD_{ref} and OD are the optical densities, Φ_{ref} and Φ are the quantum yields, and A_{ref}, A are the area of the fluorescence bands, each parameter for the standard (ref) and sample solution, respectively. For all electronic spectroscopic studies (absorption, fluorescence excitation and fluorescence emission) 1.0×10^{-5}M solutions of the compounds were used. Deionised and double distilled water was used for the preparation of all aqueous solutions. Since the compounds are sparingly soluble in water, their stock solutions were prepared in methanol (1.0×10^{-3}M) and required amount of these solutions were added to appropriate amount of surfactant to prepare micellar solutions in which the percentage of methanol was not more than 1%. The surfactants concentration was 1.0×10^{-2}M. All the solutions were prepared and handled under dim light conditions.

Compound **1** has been prepared earlier by the Wittig reaction of indolic ylides and benzaldehyde [14] and by tributylphosphine-mediated coupling of appropriate gramine with benzaldehyde [15]. However, we have prepared this compound by a simpler method though in low yield by the condensation of indole-3-carboxaldehyde and phenylacetic acid. In a typical preparation, indole-3-carboxaldehyde (0.8 g, 5.51 mmol) and phenylacetic acid (1.36 g, 10 mmol) were taken in distilled pyridine (10 mL). A few drops of piperidine (0.5 mL) were added and the reaction mixture was stirred continuously at 90°C for 9 h. The progress of the reaction was monitored by TLC (10% EtOAc in petroleum ether). The reaction mixture was cooled and poured to a beaker containing crushed ice. The resulting solution was treated with dilute hydrochloric acid (2N) to neutralize pyridine. This gave yellowish solid which was purified by column chromatography (silica gel, 6% EtOAc in petroleum ether), when **1** was obtained in 5% yield; m.p.: 191–193°C [Lit. [15] 192–193°C]. It showed ^{1}H NMR identical to the reported data [15]. In addition, it showed the following characteristic physico-chemical data: HPLC: R_t=9.63 min (2 mL/min EtOAc-hexane 8:100, 330 nm); UV-Vis (MeOH) $\lambda_{max,}$ 327 nm (ε, 32,510 $lmol^{-1}$ cm^{-1}); IR ν_{max} (cm^{-1}): 3,388 (–NH str), 2,921(C–H str), 1,633 (C=C str); MS m/z (% rel. int): 219 (M^+, 18).

3-[2-(4-Nitrophenyl)ethenyl-*E*]indole (**2**) was prepared as reported earlier [7] and its physico-chemical data were identical to the reported data [7]. Compound **3** was synthesized by a reaction between N-phenylsulfonylindol-3-carboxaldehyde and *p*-cyanobenzyl bromide under a modified Wittig-Horner reaction condition, wherein ethylation of indolic –NH was achieved *in situ* [16]. In a typical procedure, triethylphosphite (1.53 mL, 9 mmol) was added to *p*-cyanobenzyl bromide (0.88 g, 4.5 mmol) taken in DMF (6 mL) in 100 mL three neck round bottom flask and heated at 160°C for three hours to give the corresponding phosphonate. Then the reaction mixture was allowed to cool to room temperature and slowly added to a suspension of sodium hydride (0.43 g, 18 mmol) (pre-washed with hexane) in DMF at 0°C under nitrogen atmosphere with continuous stirring. N-Phenylsulfonylindole-3-carboxaldehyde (0.85 g, 3 mmol) taken in DMF was drop wise added to the stirring reaction mixture. The mixture was slowly brought to room temperature and stirring was allowed to continue for 7 hours. Then the reaction mixture was poured to a beaker containing crushed ice and the product was extracted with diethyl ether. The ether layer was dried with anhydrous sodium sulfate and removal of the solvent under reduced pressure gave a yellow solid, which on column chromatography on silica gel (6% EtOAc in petroleum ether) gave 3-[2-(4-cyanophenyl)ethenyl-*E*]-N-ethylindole (**3**): m.p.: 111–113°C; HPLC: R_t=9.7 min (2 mL/min EtOAc-hexane 8:100, 368 nm); UV-vis (MeOH): λ_{max}

368 nm (ε, 34,920 $lmol^{-1}cm^{-1}$); IR (KBr) ν_{max} (cm^{-1}): 3,047 (aromatic C–H str) 2,991 (C–H str) 2217.8 (CN str), 1,632 (C=C str); ^{1}H NMR ($CDCl_3$, 400 MHz) δ 7.96 (1H, d, J=8.0 Hz, C_4–H), 7.58 (2H, d, J =8.0 Hz, *ortho* to –CN), 7.53 (2H, d, J=8.0 Hz, *meta* to CN), 7.41 (1H, d, J= 16.0 Hz, –CH=CH–ArCN), 7.37 (1H, d, J=8.0 Hz, C_7–H), 7.35 (1H, S, C_2–H), 7.26 (2H, m, C_5–H and C_6–H), 7.04 (1H, d, J=16.0 Hz, –CH=CH–ArCN), 4.17 (2H, q, J= 8.0 Hz, N–CH_2CH_3), 1.49 (3H, t, J =8.0 Hz, N–CH_2CH_3). MS: m/z (% rel. int) 273 (MH^+, 100).

For the preparation of compound **4**, a procedure similar to the one described above for compound **3** was employed, excepting that in this case the N-phenylsulfonylindole-3-carboxaldehyde was reacted with purified diethyl-*p*-cyano-benzyl phosphonate. The rest of the procedure was same. (**4**): m.p.: 190–191°C; UV-vis (MeOH): λ_{max} 365 nm (ε, 38,520 $lmol^{-1}cm^{-1}$) ; IR (KBr) ν_{max} (cm^{-1}): 3,300 (–NH str), 2,225 (CN str), 1,630 (C=C str); ^{1}H NMR ($CDCl_3$, 400 MHz): δ 8.30 (1H, s, br, –NH), 7.99 (1H, d, J=8.0 Hz, C_4–H), 7.62 (2H, d, J = 8.0 Hz, *ortho* to –CN), 7.57 (2H, d, J = 8.0 Hz, *meta* to –CN), 7.45 (1H, d, J=16.4 Hz, –CH=CH–ArCN), 7.44 (1H, s, C_2–H), 7.43 (1H, d, J=8.0 Hz, C_7–H), 7.24–7.28 (2H, m, C_5–H, and C_6–H), 7.11 (1H, d, J=16.4 Hz, –CH=CH–ArCN); MS: m/z (% rel. int.) 245 (MH^+, 100)

Results and discussion

Absorption and fluorescence emission studies in homogeneous media of organic solvents

The UV-visible and fluorescence spectral data of **1**–**4** in organic solvents are summarized in Table 1. As compared to the parent compound 3-styrylindole **1**, which absorbs maximally at 322–330 nm, the $\lambda_{ab\ max}$ of the other substituted 3-styrylindoles **2**–**4** are red-shifted. Large red shift is observed for **2** in which the electron-withdrawing nitro group is on the *para* position of the aromatic ring. The $\lambda_{ab\ max}$ of **2** is significantly red shifted (ca. 25 nm) as the solvent polarity is increased from *n*-hexane to methanol. Figure 2 shows the absorption spectra of **2** in organic solvents of different polarity. The other compounds exhibited only moderate solvatochromic red shift of 6 nm–10 nm as the solvent polarity is increased. The red shift in the absorption maximum of these compounds is attributed to the mesomeric effects of the substituent present on the *para* position of the aromatic ring.

In contrast to a rather moderate solvent polarity effect on the $\lambda_{ab\ max}$, marked influence of solvent polarity on their $\lambda_{f\ max}$ is observed. Fluorescence spectra of **2**–**4** in organic solvents of various polarities are presented in Figs. 2 and 3. Maximum red shift of 129 nm in $\lambda_{f\ max}$ is observed for compound **2** as the solvent is changed from non-polar *n*-hexane to polar aprotic acetonitrile. The next maximum red shift of 59 nm was observed for compound **3** in which the cyano group is present as acceptor on the *para* position of the aromatic ring and the hydrogen of the indole nitrogen is replaced by ethyl group. Compound **1** exhibited only a 26 nm red shift in its $\lambda_{f\ max}$.

The Stokes' shift of the nitro substituted compound **2** is relatively large and increases with solvent polarity. The dependence of the Stokes' shift on the solvent polarity is correlated with solvent polarity parameters like Dimroth parameter $E_T(30)$ [17] (Fig. 4A) and Kamlet-Taft π* scale [18]. It is observed that the Stokes' shift increases linearly with the increase in solvent polarity for compounds **1**–**4**.

Table 1 UV-vis absorption and fluorescence data of styrylindoles (**1**–**4**) in homogenous media (For **2**, see Ref. [7])

Compound	Solvent	$\lambda_{ab\ max}$ (nm)	$\lambda_{f\ max}$ (nm)	$\lambda_{ex\ max}$ (nm)	Stokes' shift (cm^{-1})	Φ_f±0.002
1	*n*-Hexane	322	382	330	4,877	0.0016
	1,4-Dioxane	328	384,404(s)	332	4,446	0.0028
	THF	330	403	336	5,489	0.0013
	MeCN	326	407	332	6,104	0.0010
	MeOH	327	408	334	6,071	0.0012
3	*n*-Hexane	360	410,430(s)	365	3,387	0.0020
	1,4-Dioxane	367	434	366	4,206	0.0045
	THF	370	447	384	4,655	0.0038
	MeCN	368	469	379	5,851	0.0035
	MeOH	368	464	380	5,622	0.0037
4	*n*-Hexane	354	395, 411	351	3,918	0.0013
	1,4-Dioxane	360	427	360	4,358	0.0038
	THF	364	434	350	4,431	0.0031
	MeCN	359	454	360	5,829	0.0040
	MeOH	364	456	364	5,543	0.0043

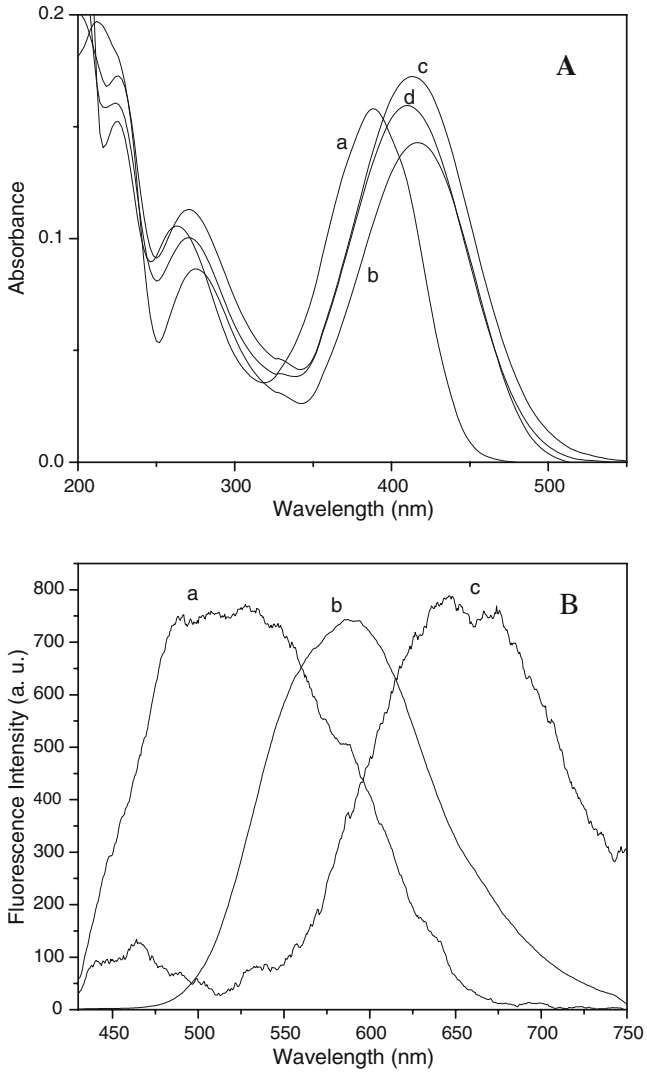

Fig. 2 (**A**) UV-visible absorption spectra of **2**. *a*) *n*-hexane; *b*) THF; *c*) acetonitrile and *d*) methanol. (**B**) Fluorescence spectra of **2**. *a*) *n*-hexane; *b*) THF and *c*) acetonitrile

The solvatochromic shift of fluorescence maxima of these compounds were also analyzed using the Lippert-Mataga equation [19]: $\nu_a - \nu_f = \{[2(\mu_e - \mu_g)^2 / hca^3] F(\varepsilon,\eta)\}$ where $\nu_a - \nu_f$ is the Stokes' shift, μ_e and μ_g are excited and ground state dipole moments, respectively. $\mu_e - \mu_g = \Delta\mu$ is change in dipole moment, h is Planks' constant, c is the velocity of light, a is the Onsager radius, and $F(\varepsilon, \eta) = \Delta f$ is the solvent polarity determining factor. $\Delta f = [(\varepsilon - 1) / (2\varepsilon + 1)] - [(\eta^2 - 1) / (2\eta^2 + 1)]$, where ε is the dielectric constant and η is the refractive index of the solvent. The Onsager radius for these compounds was taken as 7.3 Å which is a reported value for stilbene compounds (N,N-dimethylamino-*p*-nitrostilbene) [20]. The plots of Stokes' shift vs. solvent polarity parameter, Δf, are shown in Fig. 4B. From the slopes of these plots using the Lippert-Mataga equation [19], the change in dipole moment ($\Delta\mu$) upon excitation for **1**–**4** is calculated to be 13.1 D, 18.4 D, 18.2 D and 15.6 D, respectively. The large red shift in fluorescence emission and high change in excited state dipole moment in polar medium points towards polar nature of the emissive state of these compound, which can be due to the intramolecular charge transfer (ICT) excited state.

Spectral studies of compounds (**2**–**4**) in 1,4-dioxane-water binary mixtures and micelles

The dependence of fluorescence properties of **2**–**4** on solvent polarity prompted us to study their spectral properties in aqueous medium and CTAB, SDS and Triton-X-100 micelles. For this purpose, the electronic

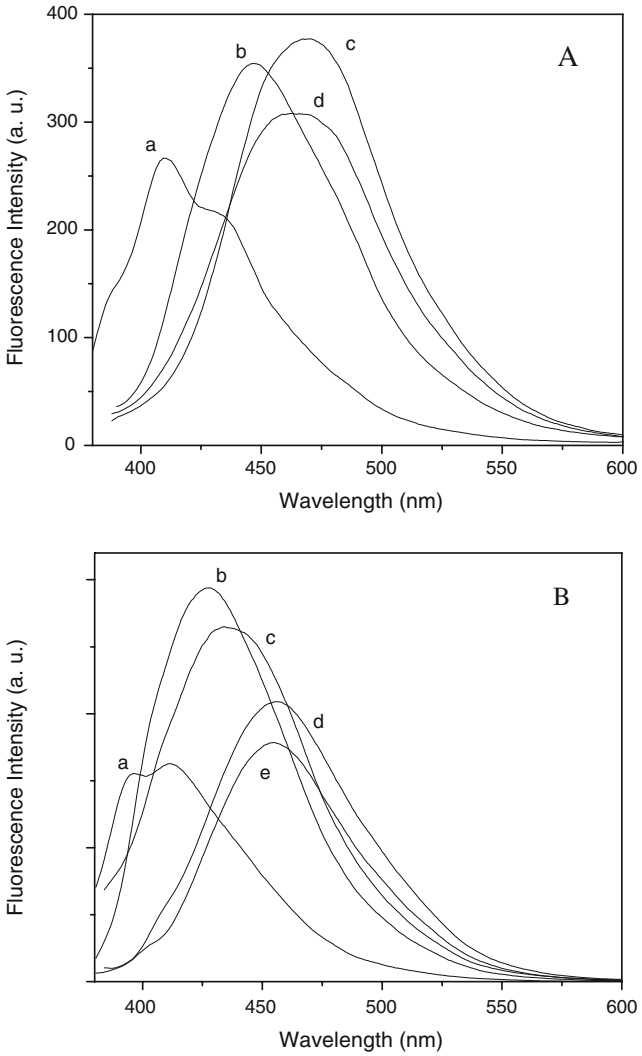

Fig. 3 (**A**) Fluorescence spectra of **3**. *a*) *n*-hexane; *b*) THF; *c*) acetonitrile and *d*) methanol. (**B**) Fluorescence spectra of **4**. *a*) *n*-hexane; *b*) 1,4-dioxane; *c*) THF; *d*) acetonitrile and *e*) methanol

absorption and fluorescence emission spectra of **2**–**4** were first examined in 1,4-dioxane-water binary mixtures. In case of compound **2**, it was observed that as the amount of water in 1,4-dioxane increased its $\lambda_{f\ max}$ gets red-shifted with drastic decrease in its fluorescence intensity. When the amount of water in 1,4-dioxane increased beyond 30% no appreciable fluorescence emission was observed for this compound. This is may be due to formation of hydrogen bond with water molecules. In the case of compounds **3** and **4**, the $\lambda_{f\ max}$ get red-shifted as the amount of water in 1,4-dioxane is increased and at the same time their fluorescence intensity increased (Fig. 5). The 526 nm emission of **2** in 1,4-dioxane is shifted to 590 nm when the 1,4-dioxane contained 30% water. Similarly 434 nm and 428 nm fluorescence of **3** and **4** in 1,4-dioxane, respectively, shifted to 486 nm and 473 nm in water. Thus, the fluorescence of these compounds is highly shifted as the water content in the 1,4-dioxane is increased. This is because of the greater stabilization of highly polar excited states of **2**, **3** and **4** ($\Delta\mu$ =18.4 D, 18.2 D and 15.6 D, respectively) by the more polar water molecules. The dielectric constants (ε) and $E_T(30)$ values of 1,4-dioxane-water mixtures are known in literature [21] and the $\lambda_{f\ max}$ of **2**–**4** were plotted against the dielectric constants (ε) and $E_T(30)$ values of 1,4-dioxane-water mixtures (Fig. 6). As can be seen from Fig. 6B, the $\lambda_{f\ max}$ of **2**–**4** correlate linearly with $E_T(30)$ values of the 1,4-dioxane-water mixture (**2**: R^2=0.946, **3**: R^2 = 0.989 and **4**: R^2 = 0.978). The variation of $\lambda_{f\ max}$ of the 3-styrylindoles with the dielectric constant (ε) and $E_T(30)$ values of the 1,4-dioxane binary mixtures is used for probing the micropolarity of the micelles in the following section.

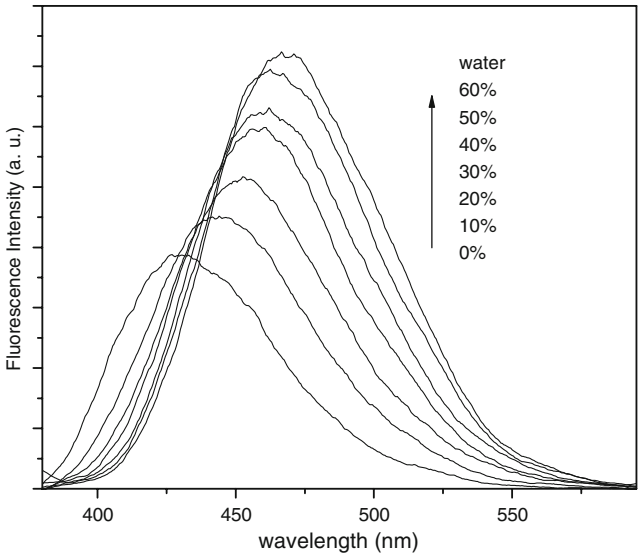

Fig. 5 Fluorescence emission spectra of **4** in 1,4-dioxane-water binary mixtures. The percentage of water (v/v %) are shown in the figure

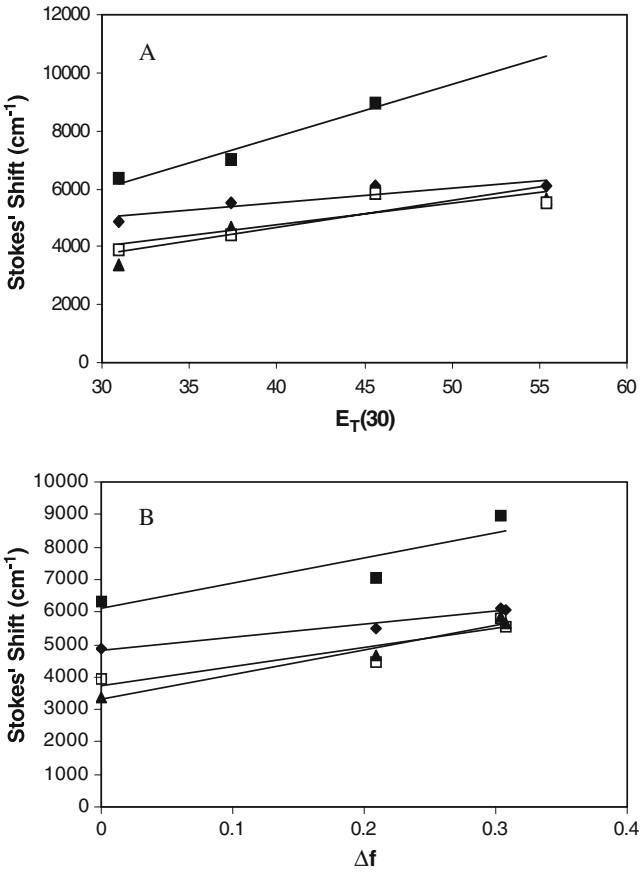

Fig. 4 (**A**) Plot of Dimroth empirical solvent parameter E_T (30) *vs*. Stokes' shift of **1** (♦), **2** (■), **3** (▲) and **4** (□). (**B**) Lippert-Mataga plot of Stokes' shift *vs*. solvent polarity Δf of **1** (♦), **2** (■), **3** (▲) and **4** (□)

Polarity of the micellar environments around the probes

The absorption and fluorescence data of **2**–**4** in CTAB, SDS and Triton-X-100 micelles are summarized in Table 2. As can be seen from the data, the $\lambda_{f\ max}$ of **1**–**4** in the micelles is blue-shifted as compared to their $\lambda_{f\ max}$ in polar solvents and water. The fluorescence emission spectra of **2**–**4** were also recorded as a function of concentration of surfactants (CTAB, SDS and Triton-X-100). The gradual increase of surfactant concentration causes a blue shift in $\lambda_{f\ max}$ and enhancement in fluorescence intensity (some representative spectra are shown in Fig. 7).

The spectral shifts and enhancement of the fluorescence intensities can be explained in terms of binding of these compounds to a less polar site of the micelles. In view of a possible ICT nature of the excited state of **2**–**4**, it is expected that the lowering of the polarity of the medium will destabilize the excited state more than the ground state.

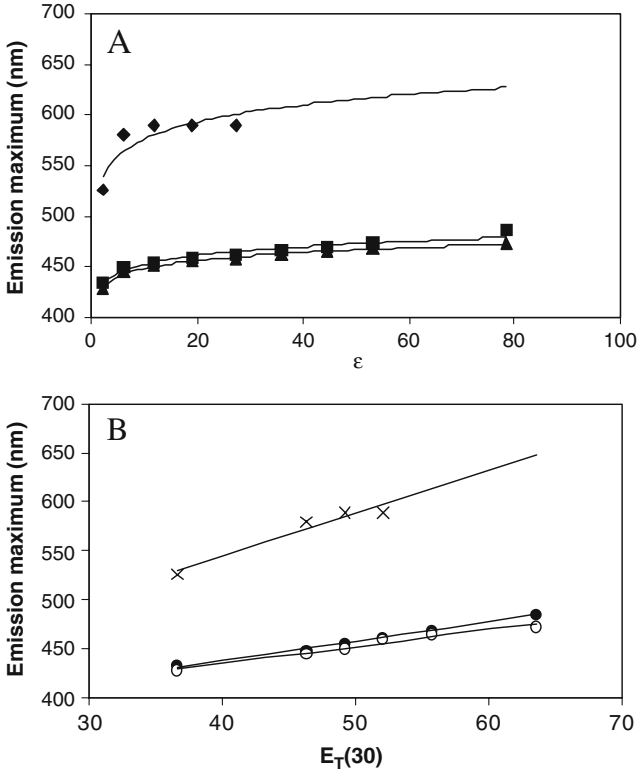

Fig. 6 (**A**) Plots of the fluorescence emission maxima of **2** (◆), **3** (■) and **4** (▲) *vs*. dielectric constant (ε) of 1,4-dioxane-water mixtures. (**B**) Plots of the fluorescence emission maxima of **2** (x), **3** (•) and **4** (◦) *vs*. $E_T(30)$ of 1,4-dioxane-water mixtures

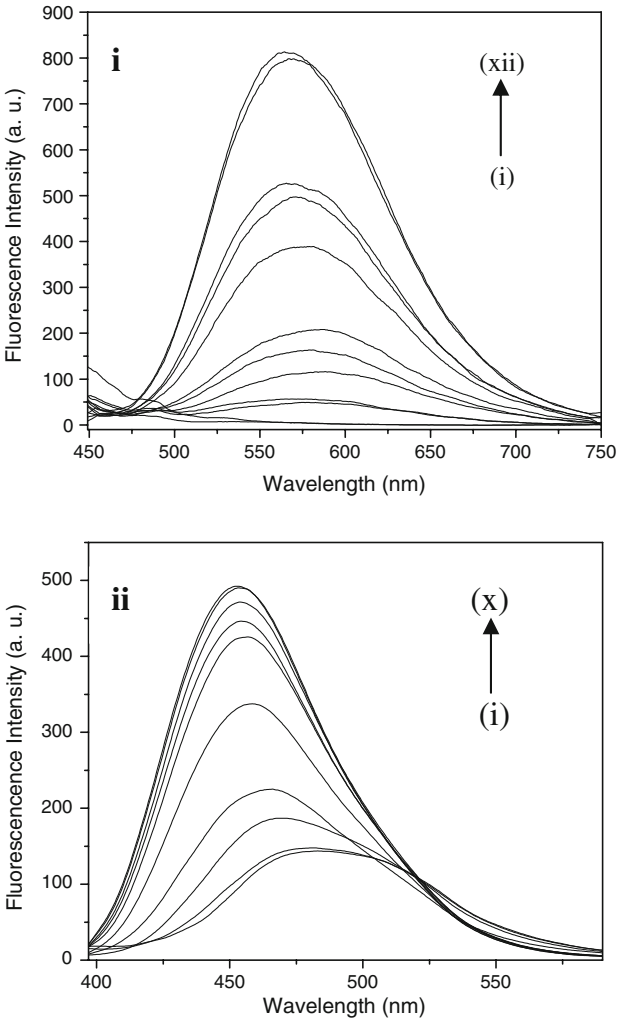

Fig. 7 (**i**) Fluorescence emission spectra of **2** as a function of TX-100 concentration (λ_{exc}=427 nm). Curves (i) – (xii) correspond to 0.0, 0.1, 0.2, 0.25, 0.3, 0.35, 0.4, 0.6, 0.8, 1.0, 5.0 and 10.0 mM. (**ii**) Fluorescence emission spectra of **3** as a function of TX-100 concentration (λ_{exc}=377 nm). Curves (i)-(x) correspond to 0.0, 0.1, 0.25, 0.3, 0.4, 0.6, 0.8, 1.0, 3.0, 5.0 mM

As a result, the energy gap between the excited state and the ground state increases. Thus, the $\lambda_{f\ max}$ is shifted to the blue region. The dielectric constant (ε) and $E_T(30)$ of the solubilization site of the 3-styrylindoles in CTAB, SDS and Triton-X-100 were determined by perusing Fig. 6 and comparing it with the fluorescence maximum in micellar

Table 2 UV-vis absorption and fluorescence data of 3-styryl indoles (**1**–**4**) in microheterogemeous media of micelles

Compound	Media	$\lambda_{ab\ max}$ (nm)	$\lambda_{f\ max}$ (nm)	$\lambda_{ex\ max}$ (nm)	Stokes' shift (cm^{-1})	Φ_f±0.002
1	CTAB	333	396	337	4,777	0.0050
	SDS	329	402	333	5,519	0.0027
	TX-100	334	392	338	4,429	0.0086
2	CTAB	432	529	406	4,244	0.0087
	SDS	431	529	406	4,298	0.0046
	TX-100	427	566	422	5,751	0.2287
3	CTAB	380	460	389	4,576	0.0134
	SDS	379	466	387	4,925	0.0118
	TX-100	378	453	387	4,379	0.0179
4	CTAB	372	460	376	5,142	0.0108
	SDS	369	464	366	5,548	0.0115
	TX-100	372	451	382	4,708	0.0179

Table 3 Polarity parameters, ε and $E_T(30)$, critical micelle concentration (CMC) and binding constant (K) of micelles as determined using 3-styrylindoles probes **2**–**4**

Probe	Micelle	ε	$E_T(30)$ (kcalmol^{-1})	CMC (10^{-3}M)	K (M^{-1})
2	CTAB	–	–	–	–
	SDS	–	–	–	–
	TX-100	6.6	44.8	0.25	4.32×10^5
3	CTAB	20	51.1	1.95	2.23×10^4
	SDS	30	54.1	5.0	2.45×10^4
	TX-100	10.6	47.5	0.22	6.62×10^5
4	CTAB	31.6	54.4	0.6	1.50×10^4
	SDS	40	56.7	6.5	6.56×10^4
	TX-100	15	49.2	0.25	4.14×10^6

solutions. The $E_T(30)$ values were calculated by using the correlation obtained from the linear best fit of the data in 1,4-dioxane-water binary mixtures (Fig. 6B). The equations are given below:

$$\text{Compound } \mathbf{2} : \lambda_{f\,max} = 4.409\ E_T(30) + 368 \quad R^2 = 0.946 \tag{2}$$

$$\text{Compound } \mathbf{3} : \lambda_{f\,max} = 1.954\ E_T(30) + 360 \quad R^2 = 0.989 \tag{3}$$

$$\text{Compound } \mathbf{4} : \lambda_{f\,max} = 1.736\ E_T(30) + 365 \quad R^2 = 0.978 \tag{4}$$

The dielectric constants and $E_T(30)$ values of the micelles as determined by probes **2**–**4** are given in Table 3. It can be observed that the 3-styrylindoles are located in the less polar region in neutral micelle (Triton-X-100) as compared to ionic micelles (CTAB and SDS).

Estimation of probe-micelle binding constant

The binding constants (K) of **2**–**4** with micelles have been determined from the fluorescence intensity data following the method described by Almgren *et al.* [22]. This model assumes a Poisson distribution of the probes among the micelles instead of the concentration of the empty micelles. According to this the equilibrium ratio can be obtained by changing the proportions of dissolved to 'free' solute from the following relationship: $(I_\alpha - I_0) / (I_t - I_0) = 1 + (K_{eq}[M])^{-1}$, where I_0, I_t, and I_α are the relative fluorescence intensities of the fluorophore in the absence of surfactant, at an intermediate surfactant concentration and under conditions of complete solubilization, respectively, and [M], the total concentration of the micelle, is calculated using [M]=(S−CMC) / N, where S represents the surfactant concentration and N is the aggregation number of the micelle. We used this method to estimate the binding

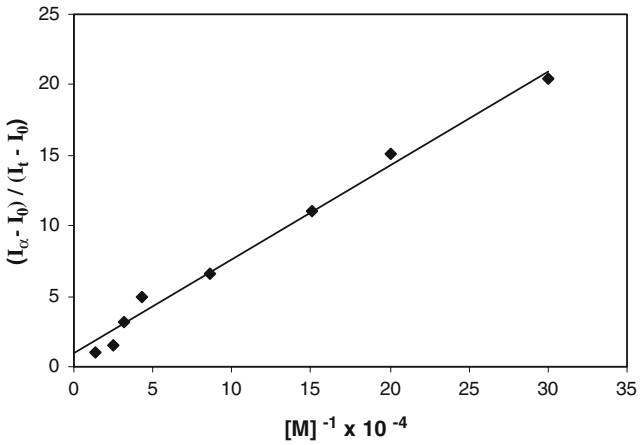

Fig. 8 A plot of $(I_\alpha - I_0)$ / $(I_t - I_0)$ vs. $[M]^{-1}$ in CTAB using **4** as fluorescent probe

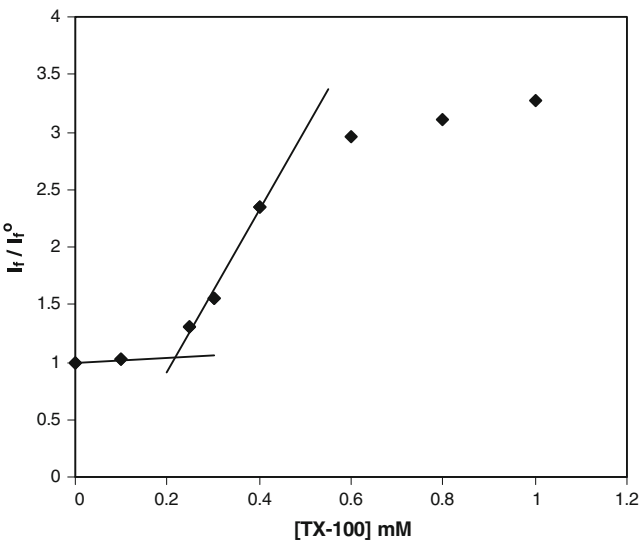

Fig. 9 A plot of relative fluorescence intensity of **3** as a function of TX-100 concentration in aqueous solution

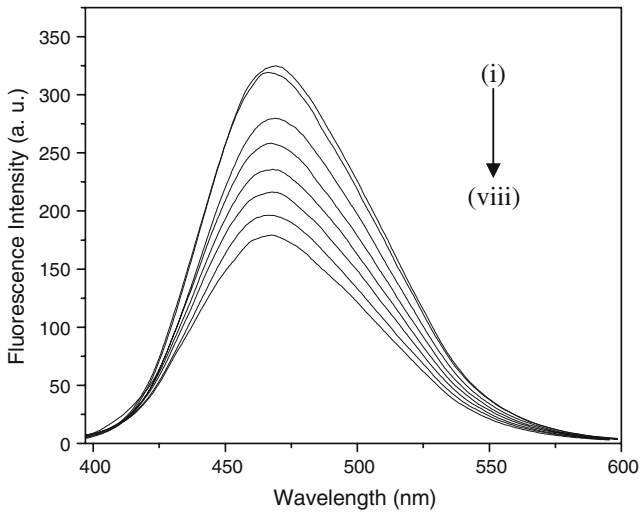

Fig. 10 Fluorescence quenching of **3** by Cu^{2+} in 0.01 M SDS. Curves (i)–(viii) correspond to 0.0, 0.99, 2.91, 5.66, 9.09, 13.04, 17.35, and 21.67 ($\times 10^{-5}$M)

constants for the association of the styrylindoles with the micelles, because the fluorescence intensity of the probes in water and in micellar environment differ significantly. The following values of N are used for the calculation of [M]: 62, 60 and 143 for SDS, CTAB and Triton-X-100, respectively [23]. The plots of $(I_\alpha - I_0)$ / $(I_t - I_0)$ against $[M]^{-1}$ have been found to be linear, and a representative plot is given in Fig. 8. The binding constants were determined from the slopes of the plots and they are given in Table 3. Relatively large binding constants for **2**, **3** and **4** with Triton-X-100 as compared to CTAB and SDS were obtained.

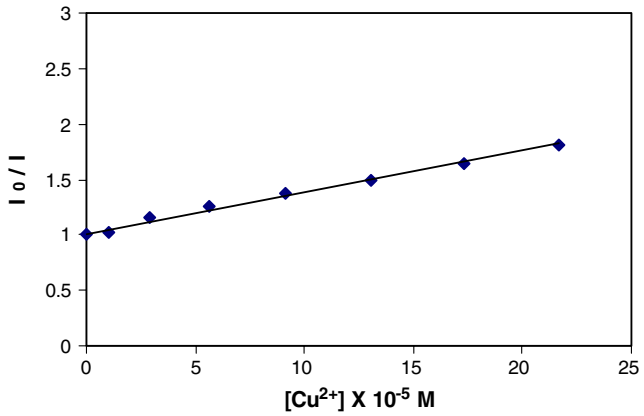

Fig. 11 A plot of the relative fluorescence intensity (I_0 / I) of **3** in micellar environment (SDS, 10^{-2}M) as the function the concentration of Cu^{2+}

Table 4 Quenching constants of 3-styrylindoles (**1**–**4**) in aqueous and micellar media

Compound	Quencher	Ksv / M^{-1}			
		CTAB	SDS	TX-100	Water
1	I^-	67.2	–	15.9	60.9
	Cu^{2+}	–	7,110	12.2	41.8
2*	I^-	–	–	8.6	–
	Cu^{2+}	–	–	8.3	–
3	I^-	198.7	–	39.7	154.4
	Cu^{2+}	–	3,830	40.8	83.6
4	I^-	121.6	–	24.7	94.4
	Cu^{2+}	–	2,900	20.5	48.4

*Negligible fluorescence in SDS and CTAB and not fluorescent in water.

Determination of critical micelle concentration (CMC)

Addition of surfactants to aqueous solutions of **2**, **3** and **4** is associated with a blue shift of the fluorescence spectrum and an increase in fluorescence intensity. This indicates the passage of the fluorophore from polar aqueous medium to a less polar site in the micellar environment. The spectral shift and enhancement are noticeable only beyond a certain critical concentration of the surfactants *i.e.* critical micelle concentration (CMC). A typical plot of relative fluorescence intensity (I_f / I_f^0) of **3** vs. Triton-X-100 concentration is given in Fig. 9. The calculated CMC values of the three micelles are collected in Table 3. These CMC values are in fair agreement with literature values 0.92 mM, 8 mM and 0.26 mM for CTAB, SDS and TX-100, respectively [2]. However, the CMC of CTAB obtained using **3** is slightly higher than the literature value.

Fluorescence quenching studies and location of **2**, **3**, and **4** in micelles

We have examined the fluorescence quenching behavior of **2**, **3**, and **4** in aqueous solution and micellar media towards ionic quenchers, I^- and Cu^{2+}, which are capable of quenching fluorescence of molecules located either in the aqueous medium or in the water accessible interfacial region of micelles. Depending on the micellar charge, we have used either one or both the quenchers for our study. The fluorescence quenching was analyzed by the Stern-Volmer equation [1], $I_0 / I = 1 + K_{SV}[Q]$, where I_0 and I are the fluorescence intensities of the fluorophore in the absences and presence of quencher, respectively, K_{SV} is the Stern-Volmer quenching constant and $[Q]$ is the

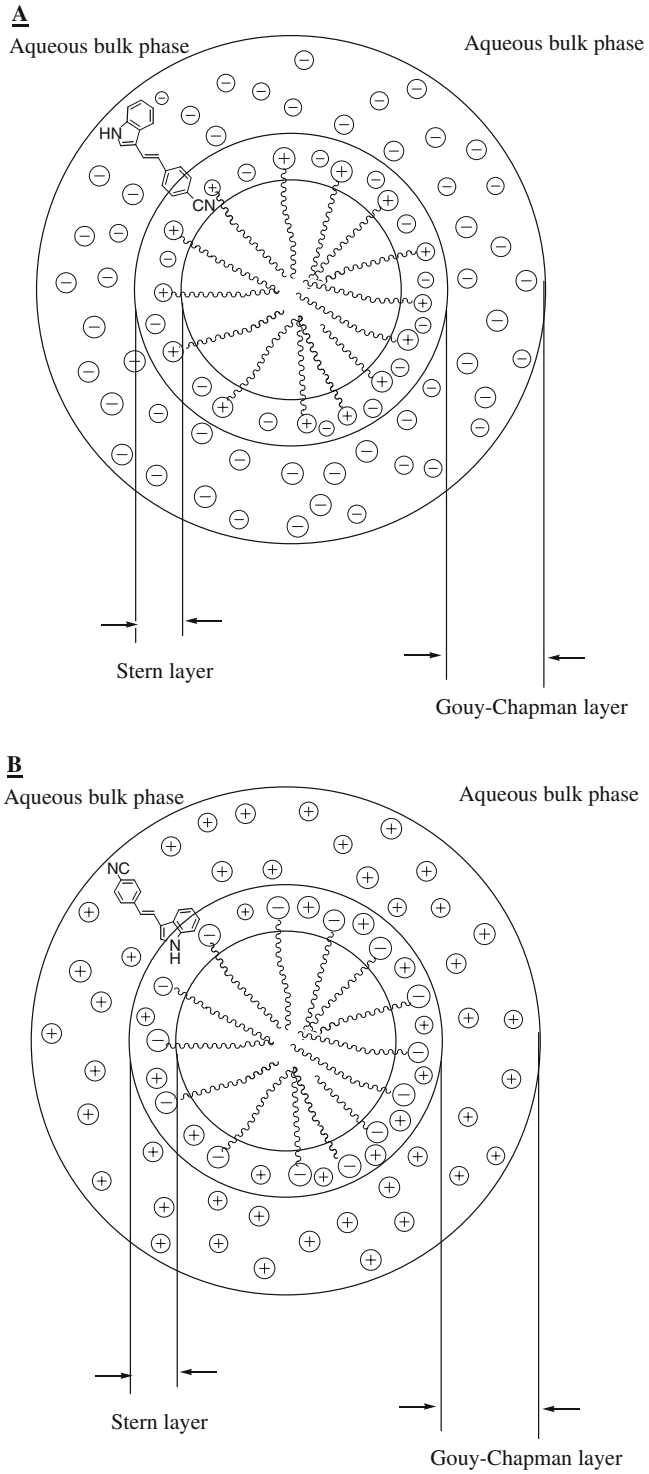

Fig. 12 Location site of **4** in aqueous solution of: (A) cationic micelle (CTAB) and (B) anionic micelle (SDS)

concentration of quencher. The fluorescence quenching of **2**, **3**, and **4** in micellar solutions and water was carried out and the Stern-Volmer plots are found to be linear. A representative of fluorescence quenching spectra and Stern-Volmer plots are given in Figs. 10 and 11, respectively. The linearity of the quenching plots is indicative of the presence of a single class of fluorophores, all equally accessible to the quenchers. In addition to this absence of any non-linearity in the plots suggests relatively small contribution of quenching by static mechanism. The K_{SV} values of quenching are collected in Table 4.

The quenching results reveal that the quenching processes are appreciable in CTAB, SDS and Triton-X-100 (Table 4). This indicates that 3-styrylindole fluorophores do not penetrate the core of the micelles; rather they bind to the micelle-water interfacial region. This is also supported by the results obtained from determination of micropolarity of the solubilization site of the 3-styrylindoles in different micelles. The dielectric constant (ε) and $E_T(30)$ values of 3-styrylindoles (Table 3) in the micelles are higher than that in 1,4-dioxane (ε =2.2 D, $E_T(30)$=36 kcal / mol) and lower than that in water (ε = 78.4 D, $E_T(30)$=63.6 kcal / mol). These results clearly indicate that the 3-styrylindoles are located in the interfacial region of the micelles, which is pictorially represented in Fig. 12. Relatively higher quenching constants are obtained in CTAB and SDS media. This is due to the electrostatic attraction between the ionic quenchers and the charged surface of the ionic micelles, which creates a very high quencher concentration in the vicinity of the probes and causes a efficient quenching. On the other hand intermediate quenching is observed in Triton-X-100, which indicates the nonionic nature of this micelle.

Conclusions

The results of UV-visible absorption and fluorescence studies of 3-styrylindoles **2**-**4** reveal the polar nature of the singlet excited state of these compounds. This type of excited state is due to intramolecular charge transfer from donor to acceptor part of the molecules. Expectedly, their fluorescence emission properties are found to be sensitive to solvent polarities. Taking advantage of these solvent sensitive fluorescence properties of 3-styrylindoles, the micelle aggregation phenomenon in CTAB, SDS and Triton-X-100 has been studied quantitatively. The location of the 3-styrylindole fluorophors in micelle-water interface is determined by using fluorescence measurements. This study clearly showed that 3-styrylindoles **2**–**4** can serve as fluorescent probes to study organized assemblies of micelles. It also provides new directions for the development of neutral, hydrophobic fluorescence probes as reporters of the microenvironments of organized assemblies.

Acknowledgment Financial support from BRNS (DAE, Government of India) for research on excited state studies of diarylpolyenes and a Research Scholarship to Mr. Abera Asefa from the Government of the Federal Democratic Republic of Ethiopia is gratefully acknowledged.

References

1. Lakowicz JR (1999) Principles of fluorescence spectroscopy, 2nd edn. Kluwer Academic/ Plenum, New York
2. Kalyanasundaram K (1987) Photochemistry in microheterogeneous systems. Academic, Orland
3. Bhattacharyya K, Chowdhury M (1993) Environmental and magnetic field effects on exciplex and twisted charge transfer emission. Chem Rev 93:507–535
4. Singh AK, Darshi M, Kanvah S (2000) αω-Diphenylpolyenes capable of exhibiting twisted intramolecular charge transfer fluorescence: a fluorescence and fluorescence probe study of nitro- and nitrocyano-substituted 1, 4-diphenylbutadienes. J Phys Chem A 104:464–471
5. Szydlowska I, Kyrychenko A, Nowacki J, Herbich J (2003) Photoinduced intramolecular electron transfer in 4-dimethylaminopyridines. Phys Chem Chem Phys 5:1032–1038
6. Davis R, Das S, George M, Druzhinin S, Zackariasse KA (2001) Intramolecular charge transfer and photochemical isomerization in donor/acceptor-substituted butadienes. J Phys Chem A 105:4790–4798
7. Singh AK, Hota PK (2006) Fluorescence and photoisomerization studies of *p*-nitrophenyl-substituted ethenylindoles. J Phys Org Chem 19:43–52
8. Singh AK, Hota PK (2005) Absorption and fluorescence spectral properties of donor-acceptor ethenes bearing indole and p-nitrophenyl substituents. Res Chem Intermed 31:85–101
9. Rettig W (1986) Charge separation in excited states of decoupled systems - TICT compounds and implications regarding the development of vision and photosynthesis. Angew Chem In Ed Engl 25:971–988
10. Guillaume BCR, Yogev D, Fendler JH (1991) Twisted intramolecular charge-transfer emissions of fluorescence probes in didodecyldimethylammonium bromide, dioctadecyldimethylammonium bromide, and didodecyl phosphate vesicles undergoing fusion. J Phys Chem A 95:7489–7494
11. Meech SR, Phillips D (1983) Photophysics of some common fluorescence standards. J Photochem 23:193–217
12. Rabek JF (1982) Experimental Methods in Photochemistry and Photophysics, Part 2. Wiley, Chichester
13. Maus M, Rettig W (2002) The excited state equilibrium between two rotational conformers of a sterically restricted donor-acceptor biphenyl as characterized by global fluorescence decay analysis. J Phys Chem A 106:2104–2111
14. De Silva SO, Snieckus V (1974) The Wittig synthesis and photocyclodehydrogenation of 3-(2-aryl)vinylindole derivatives. Canadin J Chem 52:1294–1306
15. Low KH, Magomedov NA (2005) Phosphin-mediated coupling of gramines with aldehydes: A remarkably simple synthesis of 3-vinylindoles. Org Lett 7:2003–2005
16. Singh AK, Asefa A (2007) N-Alkylation of indole compounds in modified Wittig-Horner reaction. Synth Commun 37(9):1491–1494
17. Reichardt C (2003) Solvents and Solvent Effects in Organic Chemistry. VCH, Weineim
18. Kamlet MJ, Abboud JL, Abraham MH, Taft RW (1983) Linear solvation energy relationships. 23. A comprehensive collection of the solvatochromic parameters, π*, α and β and some methods for simplifying the generalized solvatochromic equation. J Org Chem 48:2877–2887
19. Lippert E, Luder W, Moll F, Nagele H, Boss H, Prigge H, Blankenstein IS (1961) Umwandlug von elektronenanregungsenergie. Angew Chem 73:695–706
20. Lapouyade R, Kuhn A, Letard JF, Rettig W (1993) Multiple relaxation pathways in photoexcited dimethylaminonitro- and dimethylaminocyano-stilbenes. Chem Phys Lett 208:48–58
21. Fayed TA (2004) Probing of micellar and biological systems using 2-(*p*-dimethylaminostyryl)benzoxazole an intramolecular charge transfer fluorescent probe. Colloids Surf A Physicochem Eng Asp 236:171–177
22. Almgren M, Grieser F, Thomas JK (1979) Dynamics and static aspects of solubilization of neutral arenes in ionic micellar solutions. J Am Chem Soc 101:279–291
23. Saroja G, Ramachandan B, Saha S, Samanta A (1999) The fluorescence response of a structurally modified 4-aminophthalimide derivative covalently attached to a fatty acid in homogeneous and micellar environments. J Phys Chem B 103:2906–2911